Arts & Sciences Articles   Arts and Sciences

2011

Compartmentalized Connexin 43 S-Nitrosylation/Denitrosylation Regulates Heterocellular Communication in the Vessel Wall

Brant E. Isakson

Adam C. Straub

Marie Billaud

Robin Looft-Wilson
William & Mary, rlooft@wm.edu

Follow this and additional works at: https://scholarworks.wm.edu/aspubs

Compartmentalized Connexin 43 *S*-Nitrosylation/ Denitrosylation Regulates Heterocellular Communication in the Vessel Wall

Adam C. Straub, Marie Billaud, Scott R. Johnstone, Angela K. Best, Sean Yemen, Scott T. Dwyer, Robin Looft-Wilson, Jeffery J. Lysiak, Ben Gaston, Lisa Palmer, Brant E. Isakson

Objective—To determine whether *S*-nitrosylation of connexins (Cxs) modulates gap junction communication between endothelium and smooth muscle.

Methods and Results—Heterocellular communication is essential for endothelium control of smooth muscle constriction; however, the exact mechanism governing this action remains unknown. Cxs and NO have been implicated in regulating heterocellular communication in the vessel wall. The myoendothelial junction serves as a conduit to facilitate gap junction communication between endothelial cells and vascular smooth muscle cells within the resistance vasculature. By using isolated vessels and a vascular cell coculture, we found that Cx43 is constitutively *S*-nitrosylated on cysteine 271 because of active endothelial NO synthase compartmentalized at the myoendothelial junction. Conversely, we found that stimulation of smooth muscle cells with the constrictor phenylephrine caused Cx43 to become denitrosylated because of compartmentalized *S*-nitrosoglutathione reductase, which attenuated channel permeability. We measured *S*-nitrosoglutathione breakdown and NO_x concentrations at the myoendothelial junction and found *S*-nitrosoglutathione reductase activity to precede NO release.

Conclusion—This study provides evidence for compartmentalized *S*-nitrosylation/denitrosylation in the regulation of smooth muscle cell to endothelial cell communication. (*Arterioscler Thromb Vasc Biol*. 2011;31:399-407.)

Key Words: NO ■ GSNO-R ■ connexin ■ myoendothelial junction ■ nitrosylation

Within the vessel wall of resistance arteries, coordinated vascular smooth muscle cell (SMC) and endothelial cell (EC) function is integrated by complex intercellular signaling to regulate the constriction and dilation of the artery. The anatomic structures that facilitate direct SMC and EC communication within the resistance artery are myoendothelial junctions (MEJs), which are cellular extensions from ECs or SMCs that project through the internal elastic lamina[1–3] and link the plasma membranes of the 2 different cell types together. The gap junctions (GJs) at the MEJ provide a conduit for second messenger and electric signaling between the 2 cell types.[2,4,5] For example, phenylephrine (PE) stimulation of SMCs induces inositol 1,4,5-triphosphate (IP_3) generation and an increase in $[Ca^{2+}]_i$ concentrations, constricting the artery. It is thought that the IP_3 progresses to the adjacent EC through GJs at the MEJ, initiating an increase in $[Ca^{2+}]_i$ and the release of NO to modulate the magnitude of vasoconstriction, thereby regulating the tone of the artery.[6–8] Elucidation of the mechanisms regulating this process could provide novel insight into blood pressure regulation; however, the process remains uncharacterized.

GJs are intracellular signaling channels formed by 2 hexameric hemichannels, with each adjacent cell contributing 1 hemichannel. Connexin (Cx) proteins compose the channels, of which 4 different Cxs have been identified in the vasculature, with multiple studies demonstrating a potentially important role for Cx43 at the MEJ.[9] Recent studies have demonstrated that GJ communication and trafficking of Cx43 are modulated by caveolae[10–12] and caveolin-1,[13] supporting the observation that caveolin-1 could regulate Cx43 trafficking to the MEJ.[14] In addition to regulating Cx43, caveolin-1 also regulates, mobilizes, and organizes several proteins, including endothelial NO synthase (eNOS).[14–17] Although eNOS has not been shown at the MEJ, it is possible that it resides in this location because of the caveolae-rich environment.

NO participates in a plethora of physiological functions within the vessel wall, including vasodilation[18] and posttrans-

lational protein *S*-nitrosylation.[19] *S*-nitrosylation has emerged as a key mechanism by which NO may influence the function of a wide array of cellular proteins by covalently modifying sulfhydryl groups on cysteine residues both in vivo and in vitro.[20,21] Despite its high ability to diffuse, growing evidence[22,23] supports the concept that NO is generated locally; however, more important, this occurs in a concentration-dependent manner to elicit specific protein *S*-nitrosylation. Indeed, maintaining a critical balance between normal physiological protein *S*-nitrosylation and protein denitrosylation is essential.[24] One enzyme involved in regulating the balance between protein *S*-nitrosylation/denitrosylation is *S*-nitrosoglutathione reductase (GSNOR).[24] GSNOR indirectly regulates the levels of *S*-nitrosylated proteins by reducing GSNO, thereby providing equilibrium between *S*-nitrosylated proteins and GSNO.[25,26] Indeed, mice deficient in GSNOR and in vitro studies have confirmed that GSNOR mediates multiple cardiovascular functions.[24,27,28]

In this study, we provide evidence of an eNOS/GSNOR axis that regulates compartmentalized *S*-nitrosylation/denitrosylation of Cx43 permeability at the MEJ, thereby altering the constriction and dilatory response of a resistance artery. We propose that the specific cellular localization of proteins capable of dynamic *S*-nitrosylation/denitrosylation may be a template for heterocellular communication in general.

Methods

The supplemental materials (available online at http://atvb.ahajournals.org) provide expanded descriptions.

Mice

Wild-type mice, strain C57Bl/6 (Taconic), GSNOR$^{-/+}$, and GSNOR$^{-/-}$ (originally described by Liu et al[24]), were all males aged approximately 8 to 10 weeks and were used according to the University of Virginia Animal Care and Use Committee (Charlottesville) guidelines.

Vessel Cannulation

Mice were euthanized with an intraperitoneal injection of pentobarbital (60 to 90 mg/kg). First-order thoracodorsal (TD) arteries, a pair of resistance arteries (diameter, approximately 245 μm) with extensive MEJs and endothelium-dependant hyperpolarization that supplies blood to spinotrapezius muscle (supplemental Figure I), were isolated for cannulation.[29,30]

Immunolabeling on Transmission Electron Microscopy Sections

TD arteries and cremaster, coronary, and mesentery vessels were isolated and processed for immunogold labeling and quantified as previously described.[31]

Cell Culture, Isolation of In Vitro MEJ Fractions, and Biotin Switch Assay

The vascular cell coculture (VCCC) was constructed as previously described.[4]

In vitro MEJ fractions were isolated from the VCCC as previously described.[31]

Isolated EC, MEJ, and SMC fractions were subjected to the biotin switch assay as previously described.[32,33]

Immunoblots, Immunostaining, and Antibodies

Proteins were resolved using 4% to 12% bis-Tris gels, transferred to nitrocellulose, and visualized and analyzed using an imager (Li-Cor Odyssey Imager), as previously described.[34]

Immunostaining on frozen sections of VCCC and HeLa cells was performed as previously described.[35] All images were captured using a confocal microscope (Fluoview 1000).

Data on antibody source, application, concentration, and company of purchase are found in supplemental Table I.

Statistics

Statistics were performed using computer software (Origin Pro 6.0). All experiments were analyzed using 1- or 2-way ANOVA, followed by the Bonferroni posttest for differences between treatments where indicated. $P<0.05$ was considered significant.

Results

NO and GJs Regulate Heterocellular Communication

As demonstrated in Figure 1A, the stimulation of a control TD artery with PE induces an initial constriction, followed by a redilation to bring the vessel back to near resting tone. We believe that this response is because of heterocellular communication between the SMCs and the ECs, specifically the generation of a second messenger by PE in SMCs (eg, IP$_3$ or constriction), which traverses GJs at the MEJ to activate eNOS in the ECs (redilation). For this reason, we initially tested a GJ inhibitor (carbenoxylone, Figure 1A) and an NOS inhibitor (L-Nitro-Arginine Methyl Ester [L-NAME], Figure 1B) and found them both capable of significantly enhancing the constriction and inhibiting the redilation response. Because these data indicated that both Cxs and eNOS might be important regulators for intercellular communication between SMCs and ECs, we used transmission electron microscopy (TEM) and quantified the amount of Cx43 and eNOS present in the TD artery (Figure 1C and 1D). Cx43 was the only Cx enriched at MEJs (supplemental Figure IIA), indicating that it is likely a major contributor of GJ heterocellular communication from SMCs to ECs. This observation was also seen at the in vitro MEJ.[31] The presence of eNOS was also localized to the MEJ (Figure 1D), a trend we found throughout vascular beds (supplemental Figure IIB). Normal rabbit serum confirmed the specificity of our gold bead staining (supplemental Figure IIC). By using the VCCC, we also identified localized eNOS to the in vitro MEJ (Figure 1E and 1F). In contrast, neuronal NO synthase expression in TD MEJs (supplemental Figure IID through IIF), inducible NO synthase (supplemental Figure IIG through III), or another vasodilatory enzyme (cystathionine, supplemental. Figure IIJ through IIL) was not detected. Last, we observed caveolin-1, a protein capable of trafficking both eNOS and Cx43,[10–17] as being localized at the MEJ in TD arteries and in the VCCC (supplemental Figure IIIA through IIIE).

Although eNOS was identified at the MEJ in vivo and in vitro, this was not indicative of its activity. Therefore, we applied L-NAME to vessels, measured resting tone in the absence of an agonist, and found a significant constriction (Figure 2A). These data coincided with the localization of phosphorylated S1177 eNOS at the MEJ in vivo and in vitro (Figure 2B and 2C) in the absence of any agonist. Phosphorylated S633 eNOS (active) was also observed at MEJs in vitro; however, phosphorylated T495 eNOS (inactive) was not observed (Figure 2D and 2E).

S-Nitrosylation of Cx43 on C271 Regulates GJ Communication

Because our ex vivo and in vitro evidence demonstrated basally active eNOS and the presence of Cx43 at the MEJ, the capacity
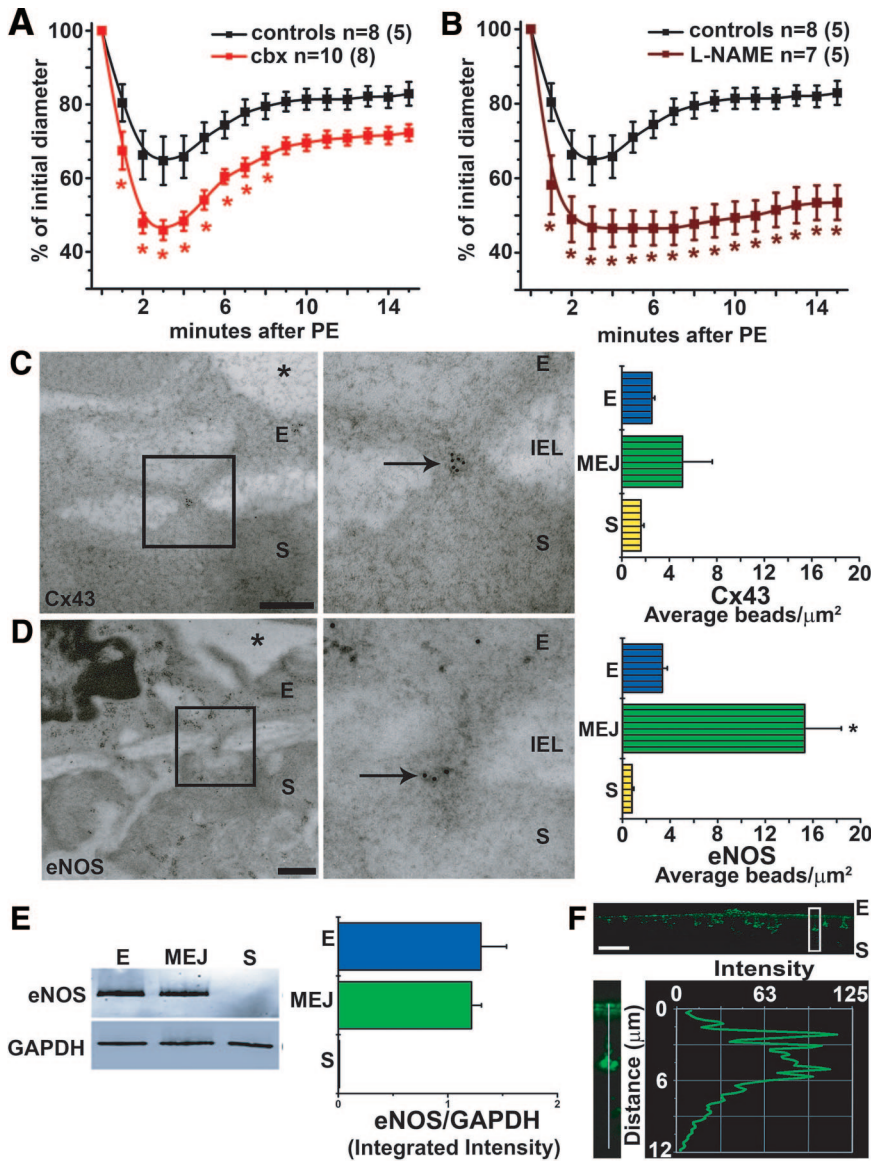
Figure 1. Vasoreactivity is altered by inhibition of GJ communication and NO correlating with Cx43 and eNOS expression at the MEJ. Mouse TD arteries were cannulated, pressurized, and stimulated with 50-μmol/L PE. A and B, Application of carbenoxolone (50 μmol/L, A) and L-NAME (100 μmol/L, B) significantly enhanced PE-induced vasoconstriction in the TD arteries. C and D, Immuno-TEM analysis of Cx43 (C) and eNOS (D) localization labeled with 10-nm gold beads (arrows) at MEJs from the TD arteries quantified the number of beads per micrometer squared. E, Isolated EC, MEJ, and SMC protein fractions from the VCCC blotted for eNOS and normalized to GAPDH. F, Immunocytochemistry of transverse sections from a VCCC were labeled for eNOS (green). The white box illustrates an enlarged MEJ with a line scan measuring fluorescence down the pore. Data are represented as the mean±SE. (C, n=8; D, n=6; E, n=4). Significant differences (*$P<0.05$) were analyzed using a 2-way ANOVA (A and B) or a 1-way ANOVA (C-E). In A and B, n is the number of vessels and the value in parentheses is the number of mice. E indicates endothelial cell; IEL, internal elastic lamina; S, smooth muscle cell; *, lumen. The scale bar in C and D is 0.5 μm; and F, 10 μm. In C through E, the open bars indicate in vitro measurements; and bars with horizontal lines, in vivo measurements.

of Cx43 to be *S*-nitrosylated was tested. Initial studies confirmed Cx43 to be constitutively *S*-nitrosylated in isolated TD arteries and at the in vitro MEJ (Figure 3A), whereas Cx40, a Cx found at the MEJ in some instances, was not *S*-nitrosylated (supplemental Figure IVA). To identify which cysteines may be responsible for *S*-nitrosylation, we used HeLa cells (which do not express Cxs or eNOS) and transfected in either Cx43 or Cx43 with all of the cysteines in the C-terminal mutated to alanines (Cx43[C260/271/298A]). After treatment of transfected HeLa cells with GSNO, *S*-nitrosylated Cx43 was only detected in the nonmutated sample (Figure 3B). This was repeated on purified Cx43 C-terminal[36] and Cx43[C260/271/298A] C-terminal peptides, which produced identical results to Cx43 proteins expressed in HeLa cells (Figure 3C). Thus, to identify whether *S*-nitrosylation was site specific, we generated Cx43 containing only 1 C-terminal cysteine. After GSNO treatment, only Cx43[C260/298A] was *S*-nitrosylated, indicating that C271 in the Cx43 C-terminal was the target for *S*-nitrosylation of Cx43 (Figure 3D). Functional changes as a result of *S*-nitrosylation were then tested in HeLa cells transfected with cysteine mutants by measuring the

extent of Ca^{2+} wave propagation after uncaging of P(4(5))-1-(2-nitrophenyl)ethyl (NPE)-IP$_3$. Calcium propagation rates were increased in response to GSNO for both Cx43 and Cx43[C260/298A] cells but unchanged in Cx43[C260/271A]-, Cx43[C271/298A]-, and Cx43[C260/271/298A]-expressing cells (Figure 3E). HeLa cells transfected without Cx43 did not propagate Ca^{2+} waves after pseudouncaging (supplemental Figure IVB). The differences in calcium wave propagation did not result from trafficking defects of the Cx43 mutations because all were effectively localized to the plasma membrane (supplemental Figure IVC through IVH). These data indicate that Cx43 and its GJ function are capable of being regulated by *S*-nitrosylation at C271.

Compartmentalized Denitrosylation of Cx43 at the MEJ

Because our previous results had demonstrated that Cx43 was extensively expressed at the MEJ and had the capacity to be *S*-nitrosylated, we tested whether PE stimulation could alter Cx43 *S*-nitrosylation. By using isolated TD arteries, we found a reduction in *S*-nitrosylation of Cx43 3 minutes after PE
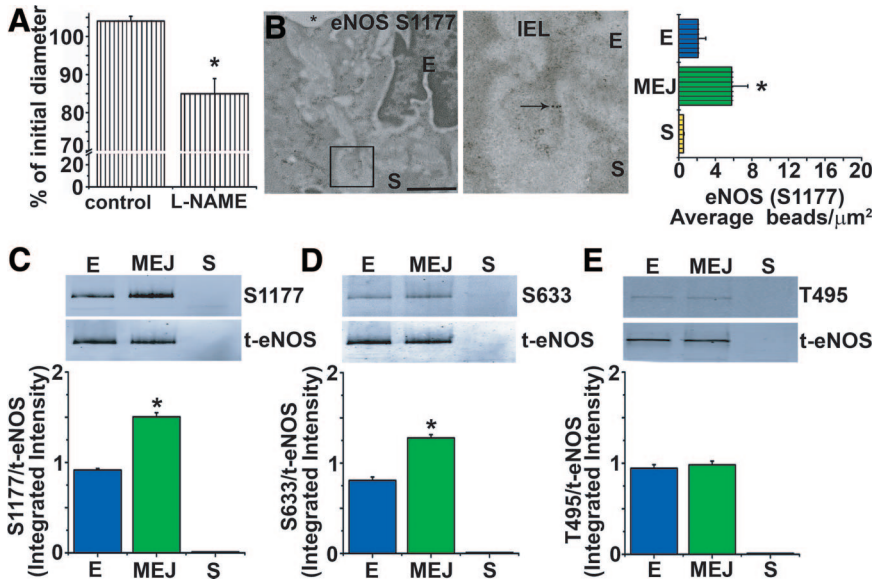
Figure 2. eNOS is differentially phosphorylated at the MEJ. Mouse TD arteries were cannulated and pressurized. A, The basal vascular tone was attenuated in the presence of L-NAME (100 μmol/L). B, Phosphorylated eNOS S1177 localization using 10-nm gold beads (arrow) in TD arteries using immuno-TEM and quantified as the number of beads per micrometer squared. C through E, Isolated EC, MEJ, and SMC fractions from the VCCC blotted for phosphorylated eNOS at sites S1177, S633, and T495 in EC, MEJ, and SMC fractions. Data are represented as the mean$\pm$SE. (A, n=5; B-E, n=4). Significant differences (*$P<0.05$) were analyzed using a 1-way ANOVA (A–D). E, endothelial cell; IEL, internal elastic lamina; S, smooth muscle cell; *, lumen. The scale bar is 0.5 μm (B). In A through E, open bars indicate in vitro measurements; and bars with horizontal lines, in vivo measurements.

stimulation, which returned to baseline after 10 minutes (Figure 4A). This result indicated that, in vivo, Cx43 at the MEJ is likely *S*-nitrosylated. Concurrent with this result, denitrosylation of Cx43 was only observed at the MEJ, and not the EC or SMC monolayer (Figure 4B), indicating a highly localized denitrosylation response (an effect identical to that seen on silver-stained gels of total *S*-nitrosylated proteins after PE stimulation) (supplemental Figure VA through VC). Neither application of 18GA (supplemental

Figure VD) nor the UV used for uncaging (supplemental Figure VE) altered Cx43 *S*-nitrosylation. To test whether denitrosylation of Cx43 correlated with changes in channel permeability, we stimulated SMCs on the VCCC with PE and then temporally uncaged NPE-IP$_3$ (Figure 4C). Under control conditions, uncaging of NPE-IP$_3$ in the SMCs elicited a robust increase in EC [Ca^{2+}]$_i$, which was significantly inhibited by the GJ blocker (18GA, Figure 4D). At 1 minute after PE stimulation, there was a significant reduction in EC
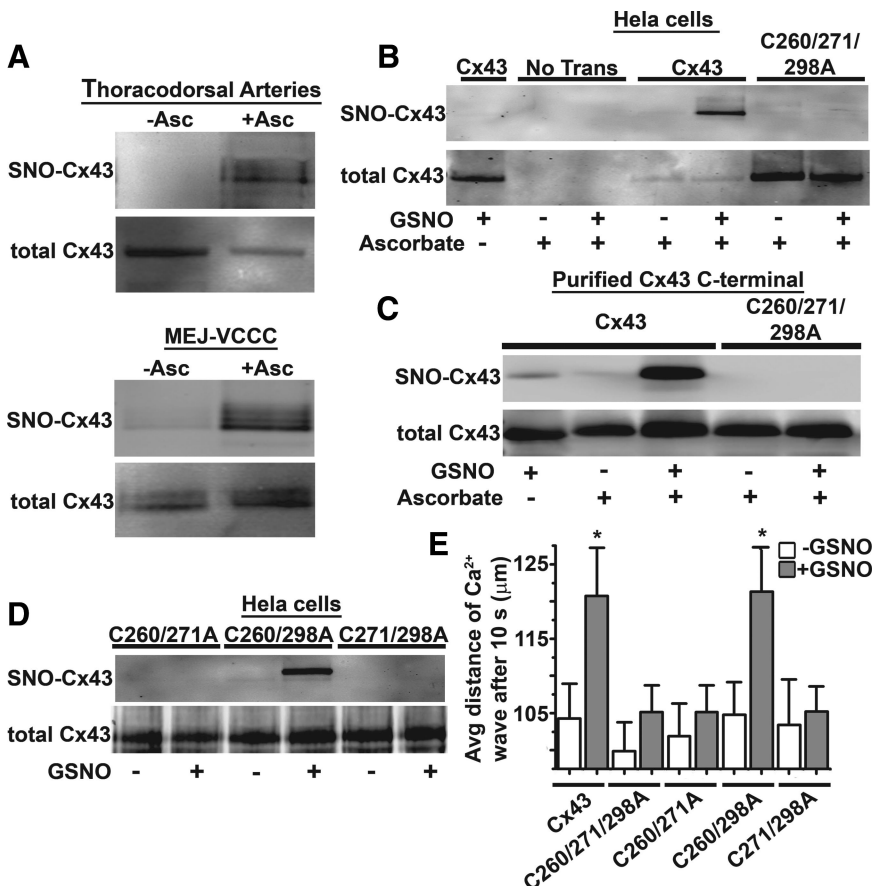

Figure 3. Cx43 is *S*-nitrosylated on cysteine 271. A, Unstimulated TD arteries or MEJ fractions analyzed by the biotin switch assay for Cx43, in which ascorbate-dependent labeling demonstrates the presence of an S-nitrosylated cysteine residue(s). B, Nontransfected and transfected HeLa cells with Cx43 or Cx43$^{C260/271298A}$ were treated with or without 100-μmol/L GSNO for 1 hour. C, Biotin switch assay of purified Cx43 C-terminal or Cx43$^{C260/271298A}$ C-terminal peptides treated with or without 100-μmol/L GSNO for 1 hour. D, HeLa cells transfected with Cx43$^{C260/271A}$, Cx43$^{C260/298A}$, or Cx43$^{C271/298A}$ and treated with 100-μmol/L GSNO for 1 hour were lysed and subjected to the biotin switch assay. E, Uncaging of NPE-IP$_3$ and analysis of calcium wave propagation and transfected HeLa cells with Cx43, Cx43$^{C260/271/298A}$, Cx43$^{C260/271A}$, Cx43$^{C260/298A}$, and Cx43$^{C271/298A}$. Data are represented as the mean$\pm$SE (n=6 to 8). Significant differences (*$P<0.05$) were analyzed using a 1-way ANOVA.
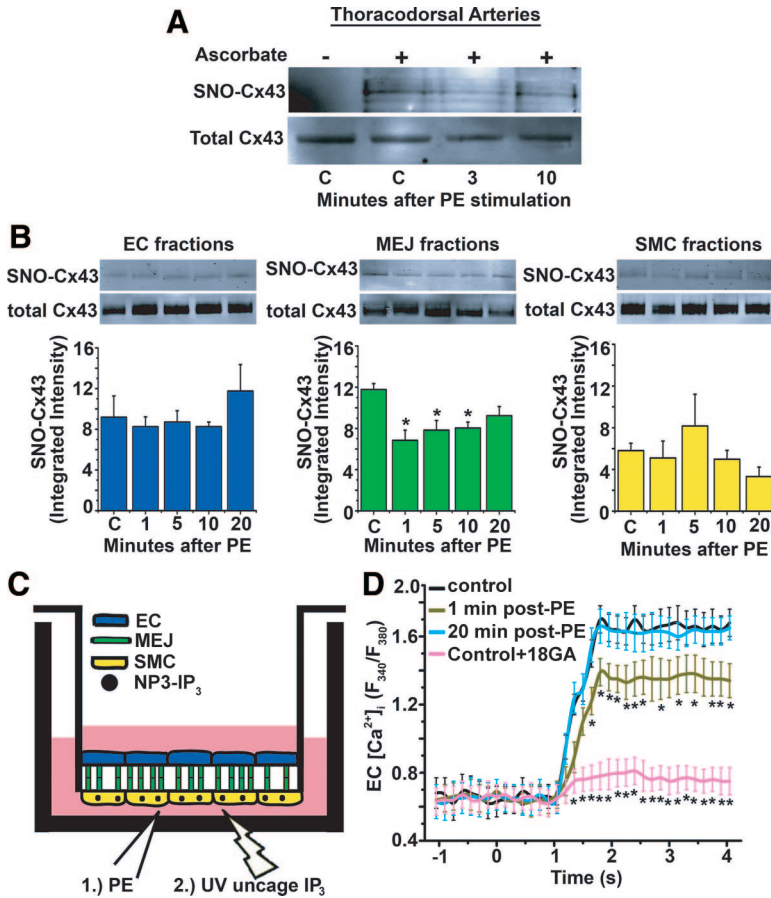
Figure 4. PE promotes denitrosylation of Cx43 and alters channel permeability. A and B, Immunoblots of isolated TD arteries or EC, MEJ, and SMC fractions identifying S-nitrosylated Cx43 using the biotin switch assay from VCCCs stimulated with PE. C, Schematic illustration of the experimental protocol used for measuring EC $[Ca^{2+}]_i$ using an initial stimulus of PE, followed by uncaging of NPE-IP$_3$ in SMCs using UV flash at specific points after PE stimulation. D, The maximum values of EC $[Ca^{2+}]_i$ were measured at control, 0, 1, and 20 minutes after PE stimulation or with the addition of 18GA. Data are represented as the mean±SE (n=3). Significant differences (*$P<0.05$) were analyzed using a 1-way ANOVA. Open bars in B indicate in vitro experiments.

$[Ca^{2+}]_i$, which returned to control levels at 20 minutes after PE stimulation. This suggested that the permeability of the GJ channel immediately after PE stimulation was decreased, which was likely because of a loss of Cx43 *S*-nitrosylation.

GSNOR Denitrosylates Cx43 at the MEJ
Because of the rapid denitrosylation of Cx43 at the MEJ on PE stimulation, we hypothesized that an enzyme capable of denitrosylating proteins may also be localized to the MEJ. Probing for GSNOR, we found the enzyme to be enriched in MEJ fractions both in vitro and in vivo (Figure 5A through 5C). In contrast, other enzymes known to denitrosylate proteins, thioredoxin-1,[37] and carboxyl reductase[38] were not present at the MEJ (supplemental Figure VIA through VIC). Next, we tested the activity of GSNOR after PE stimulation specifically in MEJ fractions and found increased activity at 1 minute, which returned to baseline after 20 minutes (Figure 5D). From the same MEJ lysates, we also measured total NO$_x$ and found a significant increase at 20 minutes compared with control and 1 minute (Figure 5E), suggesting that GSNOR activity precedes NO release. To test the effect of GSNOR activity on Cx43 denitrosylation and GJ permeability at the MEJ, we used the GSNOR inhibitor that was identified in a high-throughput screen for GSNOR inhibitors and thereby arbitrarily named C3.[28] We found a complete lack of Cx43 denitrosylation after PE stimulation (Figure 5F), a result that was similar to the result obtained using GSNOR small-interfering RNA (supplemental Figure VIIA and VIIB).

Consistent with lack of denitrosylation after inhibiting GSNOR, application of C3 did not alter GJ permeability of IP$_3$ from SMCs to ECs when compared with control (Figure 5G). TD arteries treated with C3 had an attenuated constriction after application of PE (Figure 5H). The C3 did not alter baseline artery diameter during equilibration (supplemental Figure VIIC). The GSNOR$^{-/+}$ mice were also less responsive to PE (Figure 5I), which was dependent on NOS activity and not *S*-nitrosothiols (supplemental Figure VIID). Last, the GSNOR$^{-/-}$ mice were not different from controls (supplemental Figure VIIE), a result that is due to compensatory increases in carboxyl reductase in the TD arteries (supplemental Figure VIIF).

Discussion
Highly coordinated EC and SMC cross talk regulates vessel diameter and, by extension, the blood flow rate and blood pressure. GJs positioned at the MEJ between ECs and SMCs in resistance arteries allow for signals (eg, IP$_3$) originating from 1 cell type (eg, SMCs) to rapidly diffuse to adjacent cells (eg, ECs). Although GJs have been identified at the MEJ, the specific mechanisms that regulate GJ communication at the MEJ remain largely unknown. We define a pivotal posttranslational mechanism that ECs and SMCs use to regulate heterocellular communication before, during, and after SMC constriction. Our mechanism consists of compartmentalized *S*-nitrosylation/denitrosylation of Cx43 at the MEJ to regulate the magnitude of vasoconstriction (Figure 6).
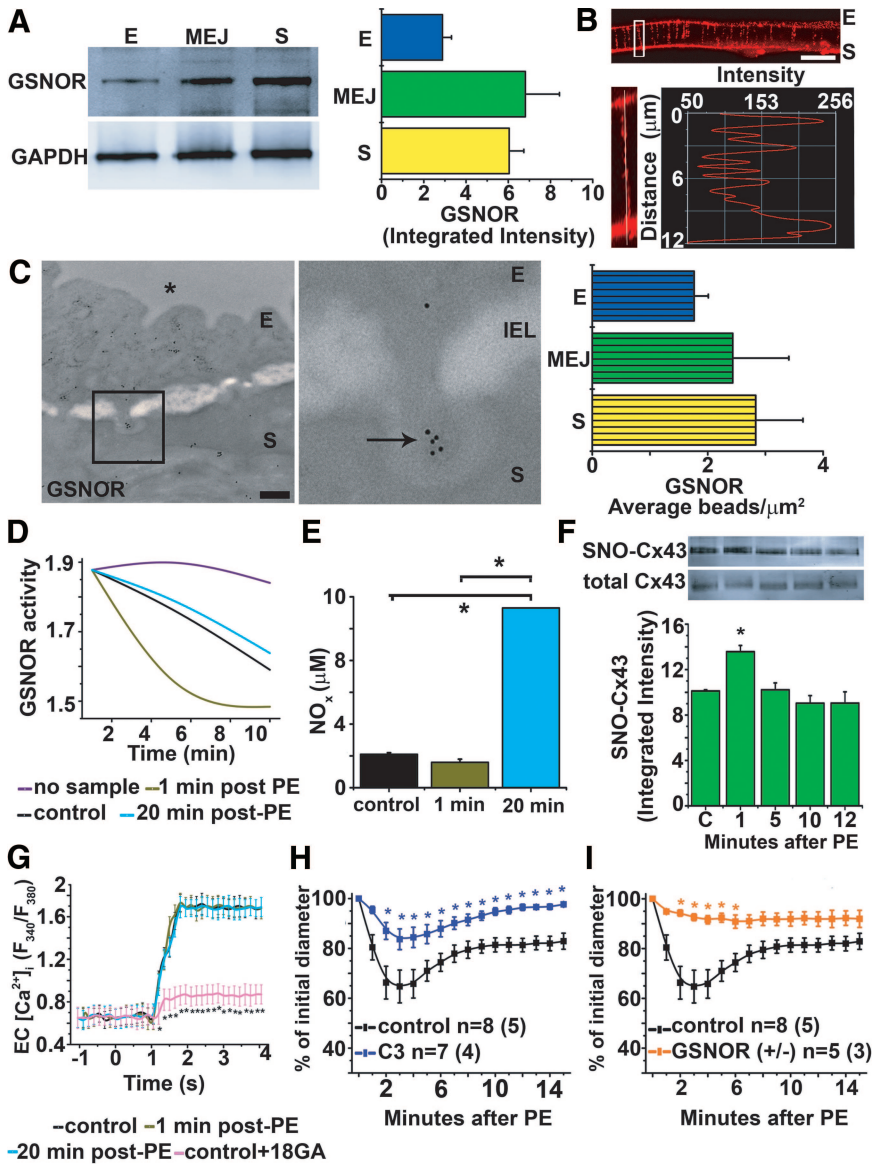
Figure 5. GSNOR regulates heterocellular communication. A, Quantitative Western blot analysis of GSNOR expression in isolated EC, MEJ, and SMC protein fractions from the VCCC normalized to GAPDH. Immunocytochemistry of transverse sections of a VCCC labeled for GSNOR (red). B, The white box illustrates an enlarged MEJ with a line scan measuring fluorescence down the pore. C, Immuno-TEM analysis of GSNOR expression labeled with 10-nm gold beads (arrows) at MEJs from the TD arteries and quantified as the number of beads per micrometer squared. D, Measurement of GSNOR activity by breakdown of GSNO in MEJ fractions at 1 and 20 minutes after PE stimulation. E, Identification of total NO_x in MEJ fractions at 1 and 20 minutes after PE stimulation. F, Immunoblot of *S*-nitrosylated Cx43 from in vitro MEJ fractions pretreated with C3 inhibitor and then stimulated with PE for 0, 1, 5, 10, and 20 minutes. G, Measurement of maximum values of EC $[Ca^{2+}]_i$ after UV uncaging is plotted at 0, 1, and 20 minutes after PE stimulation from the VCCCs pretreated with C3. H and I, Vasoconstriction response measuring percentage change of initial diameter to PE in TD arteries pretreated with C3 in wild-type mice (H) and $GSNOR^{-/+}$ mice (I). Data are represented as the mean±SE. (A, n=5; C, n=5; E, n=2; and F, n=3). In H and I, n is the number of vessels and the value in parentheses is the number of mice. Significant differences (*$P<0.05$) were analyzed using a 1-way (E-G) or a 2-way (H-I) ANOVA. The scale bar in B is 10 μm; and in C, 0.5 μm. E indicates endothelial cell; IEL, internal elastic lamina; S, smooth muscle cell; *, lumen. Open bars indicate in vitro measurements (A, E, and F); and bars with horizontal lines, in vivo measurements (C).

Several compelling observations support this discovery: (1) eNOS is enriched and active at the MEJ, (2) Cx43 *S*-nitrosylation on cysteine 271 regulates more permeable GJ channels, and (3) compartmentalized GSNOR denitrosylates Cx43, promoting less permeable GJs at the MEJ to modulate the movement of IP_3 (and potentially other factors). The cellular, pharmacological, and genetic results presented herein imply that oxidation-reduction–based protein modifications on site-specific cysteine residues are regulated in specific regions of cells to coordinate heterocellular communication.

SMC relaxation after PE-induced constriction is thought to be due to IP_3 movement from SMCs, through GJs at the MEJ, to ECs.[7] There is evidence to indicate that the IP_3 activates IP_3 receptor 1 localized to the MEJ[35] and induces an elevation of EC $[Ca^{2+}]_i$, thereby activating eNOS and releasing NO to induce subsequent vasodilation.[6,7,39] Our observation of Cx43 and active eNOS being localized to the MEJ provides the proteins necessary for a regulatable mechanism. This is supported by the observation that caveolae and caveolin-1

localize to the MEJ, thereby providing an optimal microsignaling domain whereby binding partners, including Cx43, eNOS, and many other proteins, could cluster.[10–17,35,40] Indeed, spatial partitioning of proteins within a cell provides an important level of control to ensure fidelity of cell signaling. Accumulating evidence from monolayers of cultured cells has suggested that localized eNOS could allow for NO to be generated in a specific cellular region.[22,23] It is reasonable to speculate that the active pool of eNOS we observe at the MEJ is regulating basal vascular tone and blood pressure because we show, with L-NAME, induced constriction in Figure 2. This would provide an energy-efficient mechanism to minimize NO diffusion distance to the SMCs. Thus, our identification of a pool of compartmentalized active eNOS uniquely at the MEJ throughout different vascular beds places these initial descriptive observations into a physiological context.

Our data go beyond the possibility of paracrine release of NO at the MEJ mediating the magnitude of vasoconstriction and suggest another function for the pool of localized eNOS
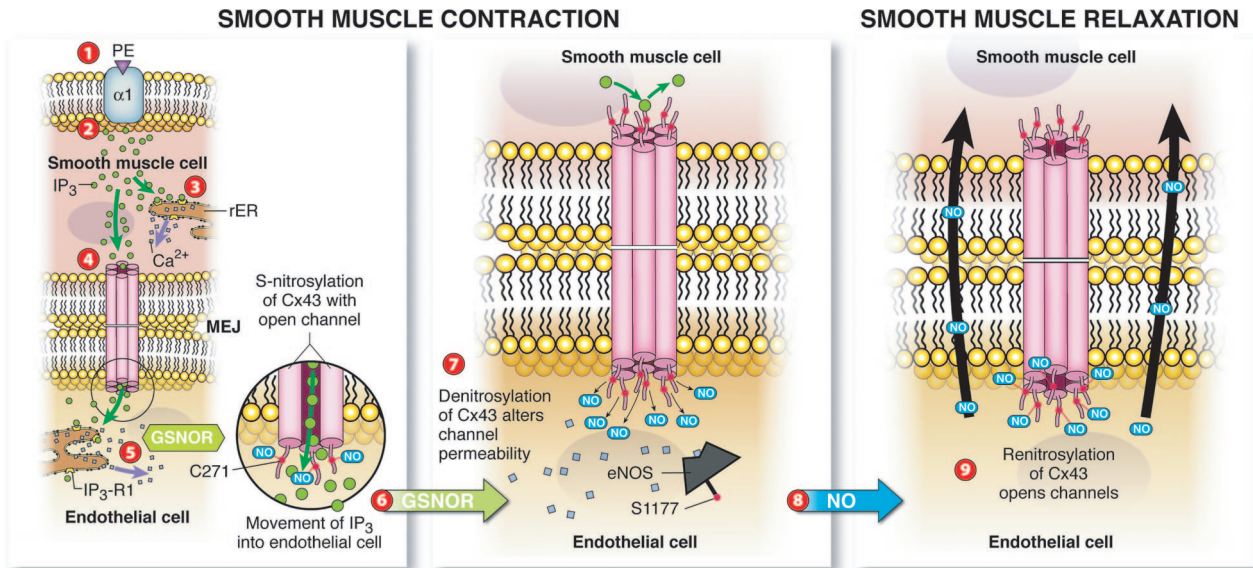
Figure 6. Schematic summary of Cx43 S-nitrosylation/denitrosylation regulating heterocellular communication in the vessel wall. Application of PE stimulates the α1 receptor (1), followed by the induction of IP_3 release in SMCs (2). The release of IP_3 activates intracellular calcium stores in endoplasmic reticulum promoting SMC contraction (3). In addition, IP_3 traverses S-nitrosylated Cx43 GJ channels at the MEJ to stimulate IP_3 receptors in ECs, inducing calcium release (5). GSNOR activity increases (6), which promotes denitrosylation of Cx43, altering channel permeability (7). Calcium and phosphorylation activate eNOS, resulting in released NO (8) to promote SMC relaxation and renitrosylation of Cx43 to open GJ channels (9).

at the MEJ (ie, regulation of GJ-mediate intracellular communication by NO). There are sporadic reports that NO could alter the function of GJ channels. For example, NO reduced Cx37 permeability and electric coupling in microvascular cells,[41,42] whereas other reports[43,44] suggest that NO enhances Cx43 electric current. However, this study used NO donors and did not explore how NOS-derived NO may posttranslationally modify the channel. It is becoming increasingly clear that S-nitrosylation is a critical posttranslational modification that regulates protein function.[20,21] Our study demonstrates that NO derived from eNOS at the MEJ constitutively S-nitrosylates Cx43 in unstimulated conditions in TD arteries and in the VCCC, thereby maintaining a more permeable GJ channel. These data correlate with recent reports[43,44] that NO acts on Cx43 hemichannels (not intact GJs) via S-nitrosylation to induce a more permeable state. Although the exact cysteines were not identified, these reports did show that the cysteines were more likely intracellular than extracellular. Therefore, we created several point mutations on the C-terminal of Cx43 and identified C271 as the critical site that significantly enhanced calcium wave propagation after IP_3 uncaging. The sum of these data indicates that Cx43 S-nitrosylation on C271 enhances permeability of the GJ channel; this can occur in a discreet cellular compartment.

Although the aggregate of our work indicated that S-nitrosylation maintained a more permeable GJ channel, it was reasonable to propose that denitrosylation of Cx43 modulated a less permeable GJ channel. Remarkably, we observed that denitrosylation after PE stimulation was confined to the MEJ rather than the EC or SMC monolayer. Of the multiple enzymes that have regulated denitrosylation, including GSNOR/GSNO,[24,45] thioredoxin-1 reductase/

thioredoxin-1,[37] and carboxyl reductase,[38] we found that GSNOR was the dominant enzyme localized at the MEJ. This was evident because GSNOR activity specifically at the MEJ increased immediately after PE stimulation, which returned to baseline after 20 minutes. Conversely, we found that NO_x was increased only at the 20-minute point, supporting the idea that GSNOR activity precedes eNOS activity. It is unknown how GSNOR activity is regulated, although one likely possibility is through a Ca^{2+}-dependent signaling pathway based on the rapid IP_3-induced increase in EC $[Ca^{2+}]_i$ and the immediacy of the effect. The pharmacological and genetic approaches in this study also support that GSNOR regulates denitrosylation at the MEJ. In cannulated vessels, C3 and GSNOR$^{-/+}$ mice both had severely attenuated constriction. It is not clear how this occurs, but based on the data from the VCCC, we believe this is due to the enhanced GJ permeability, allowing for greater IP_3 transfer from SMCs to ECs enhancing eNOS-derived NO. Previous studies[24,28] have demonstrated that inhibition of GSNOR increases S-nitrosothiols, thereby promoting SMC relaxation. However, our model system does not support this because L-NAME increased the magnitude of the constriction in cannulated vessels. Rather, these data confirm that NOS activity is a critical modulator of SMC constriction. These observations underpin the central role that compartmentalized GSNOR plays in regulating heterocellular communication in the artery wall.

In summary, results from this study emphasize the critical role that S-nitrosylation/denitrosylation contributes to heterocellular communication. Specifically, the evidence provided herein supports multiple roles for eNOS at the MEJ, including the following: (1) basal release of NO for regulating vasomotor tone and blood pressure, (2) local S-nitrosylation of

Cx43 to regulate more permeable channels, and (3) local production of NO for immediate feedback on SMCs. The presence of GSNOR provides a check on this system by inducing Cx43 denitrosylation on constriction and inducing a less permeable GJ. The results provide an investigational framework for future endeavors focusing on the eNOS/GSNOR axis as a potential therapeutic target for treating vascular pathological features, such as hypertension.

Acknowledgments

Sources of Funding

Disclosures

None.

References

1. Rhodin JA. The ultrastructure of mammalian arterioles and precapillary sphincters. *J Ultrastruct Res*. 1967;18:181–223.
2. Sandow SL, Hill CE. Incidence of myoendothelial gap junctions in the proximal and distal mesenteric arteries of the rat is suggestive of a role in endothelium-derived hyperpolarizing factor-mediated responses. *CircRes*. 2000;86:341–346.
3. Taugner R, Kirchheim H, Forssmann WG. Myoendothelial contacts in glomerular arterioles and in renal interlobular arteries of rat, mouse and Tupaia belangeri. *Cell Tissue Res*. 1984;235:319–325.
4. Isakson BE, Duling BR. Heterocellular contact at the myoendothelial junction influences gap junction organization. *Circ Res*. 2005;97:44–51.
5. Yashiro Y, Duling BR. Participation of intracellular Ca2+ stores in arteriolar conducted responses. *Am J Physiol Heart Circ Physiol*. 2003;285:H65–H73.
6. Dora KA, Doyle MP, Duling BR. Elevation of intracellular calcium in smooth muscle causes endothelial cell generation of NO in arterioles. *Proc Natl Acad Sci U S A*. 1997;94:6529–6534.
7. Isakson BE, Ramos SI, Duling BR. Ca2+ and inositol 1,4,5-trisphosphate-mediated signaling across the myoendothelial junction. *Circ Res*. 2007;100:246–254.
8. Yashiro Y, Duling BR. Integrated Ca(2+) signaling between smooth muscle and endothelium of resistance vessels. *Circ Res*. 2000;87:1048–1054.
9. Heberlein KR, Straub AC, Isakson BE. The myoendothelial junction: breaking through the matrix? *Microcirculation*. 2009;16:307–322.
10. Barth K, Gentsch M, Blasche R, Pfuller A, Parshyna I, Koslowski R, Barth G, Kasper M. Distribution of caveolin-1 and connexin43 in normal and injured alveolar epithelial R3/1 cells. *Histochem Cell Biol*. 2005;123:239–247.
11. Locke D, Liu J, Harris AL. Lipid rafts prepared by different methods contain different connexin channels, but gap junctions are not lipid rafts. *Biochemistry*. 2005;44:13027–13042.
12. Schubert AL, Schubert W, Spray DC, Lisanti MP. Connexin family members target to lipid raft domains and interact with caveolin-1. *Biochemistry*. 2002;41:5754–5764.
13. Langlois S, Cowan KN, Shao Q, Cowan BJ, Laird DW. Caveolin-1 and -2 interact with connexin43 and regulate gap junctional intercellular communication in keratinocytes. *Mol Biol Cell*. 2008;19:912–928.
14. Garcia-Cardena G, Oh P, Liu J, Schnitzer JE, Sessa WC. Targeting of nitric oxide synthase to endothelial cell caveolae via palmitoylation: implications for nitric oxide signaling. *Proc Natl Acad Sci U S A*. 1996;93:6448–6453.
15. Ghosh S, Gachhui R, Crooks C, Wu C, Lisanti MP, Stuehr DJ. Interaction between caveolin-1 and the reductase domain of endothelial nitric-oxide synthase: consequences for catalysis. *J Biol Chem*. 1998;273:22267–22271.
16. Ju H, Zou R, Venema VJ, Venema RC. Direct interaction of endothelial nitric-oxide synthase and caveolin-1 inhibits synthase activity. *J Biol Chem*. 1997;272:18522–18525.
17. Shaul PW, Smart EJ, Robinson LJ, German Z, Yuhanna IS, Ying Y, Anderson RG, Michel T. Acylation targets endothelial nitric-oxide synthase to plasmalemmal caveolae. *J Biol Chem*. 1996;271:6518–6522.
18. Palmer RM, Ferrige AG, Moncada S. Nitric oxide release accounts for the biological activity of endothelium-derived relaxing factor. *Nature*. 1987;327:524–526.
19. Lima B, Forrester MT, Hess DT, Stamler JS. S-nitrosylation in cardiovascular signaling. *Circ Res*. 2010;106:633–646.
20. Stamler JS. Redox signaling: nitrosylation and related target interactions of nitric oxide. *Cell*. 1994;78:931–936.
21. Stamler JS, Lamas S, Fang FC. Nitrosylation: the prototypic redox-based signaling mechanism. *Cell*. 2001;106:675–683.
22. Iwakiri Y, Satoh A, Chatterjee S, Toomre DK, Chalouni CM, Fulton D, Groszmann RJ, Shah VH, Sessa WC. Nitric oxide synthase generates nitric oxide locally to regulate compartmentalized protein S-nitrosylation and protein trafficking. *Proc Natl Acad Sci U S A*. 2006;103:19777–19782.
23. Qian J, Zhang Q, Church JE, Stepp DW, Rudic RD, Fulton DJ. Role of local production of endothelium-derived nitric oxide on cGMP signaling and S-nitrosylation. *Am J Physiol Heart Circ Physiol*. 2010;298:H112–H118.
24. Liu L, Yan Y, Zeng M, Zhang J, Hanes MA, Ahearn G, McMahon TJ, Dickfeld T, Marshall HE, Que LG, Stamler JS. Essential roles of S-nitrosothiols in vascular homeostasis and endotoxic shock. *Cell*. 2004;116:617–628.
25. Jensen DE, Belka GK, Du Bois GC. S-nitrosoglutathione is a substrate for rat alcohol dehydrogenase class III isoenzyme. *Biochem J*. 1998;331(pt 2):659–668.
26. Liu L, Hausladen A, Zeng M, Que L, Heitman J, Stamler JS. A metabolic enzyme for S-nitrosothiol conserved from bacteria to humans. *Nature*. 2001;410:490–494.
27. Lima B, Lam GK, Xie L, Diesen DL, Villamizar N, Nienaber J, Messina E, Bowles D, Kontos CD, Hare JM, Stamler JS, Rockman HA. Endogenous S-nitrosothiols protect against myocardial injury. *Proc Natl Acad Sci U S A*. 2009;106:6297–6302.
28. Sanghani PC, Davis WI, Fears SL, Green SL, Zhai L, Tang Y, Martin E, Bryan NS, Sanghani SP. Kinetic and cellular characterization of novel inhibitors of S-nitrosoglutathione reductase. *J Biol Chem*. 2009;284:24354–24362.
29. Billaud M, Marthan R, Savineau JP, Guibert C. Vascular smooth muscle modulates endothelial control of vasoreactivity via reactive oxygen species production through myoendothelial communications. *PLoS One*. 2009;4:e6432.
30. Saltzman D, DeLano FA, Schmid-Schonbein GW. The microvasculature in skeletal muscle, VI: adrenergic innervation of arterioles in normotensive and spontaneously hypertensive rats. *Microvasc Res*. 1992;44:263–273.
31. Heberlein KR, Straub AC, Best AK, Greyson MA, Looft-Wilson RC, Sharma PR, Meher A, Leitinger N, Isakson BE. Plasminogen activator inhibitor-1 regulates myoendothelial junction formation. *Circ Res*. 2010;106:1092–1102.
32. Jaffrey SR, Snyder SH. The biotin switch method for the detection of S-nitrosylated proteins. *SciSTKE*. 2001;2001:L1.
33. Wang X, Kettenhofen NJ, Shiva S, Hogg N, Gladwin MT. Copper dependence of the biotin switch assay: modified assay for measuring cellular and blood nitrosated proteins. *Free Radic Biol Med*. 2008;44:1362–1372.
34. Johnstone SR, Ross J, Rizzo MJ, Straub AC, Lampe PD, Leitinger N, Isakson BE. Oxidized phospholipid species promote in vivo differential cx43 phosphorylation and vascular smooth muscle cell proliferation. *Am J Pathol*. 2009;175:916–924.

35. Isakson BE. Localized expression of an Ins(1,4,5)P3 receptor at the myoendothelial junction selectively regulates heterocellular Ca2+ communication. *J Cell Sci*. 2008;121(pt 21):3664–3673.

36. Duffy HS, Sorgen PL, Girvin ME, O'Donnell P, Coombs W, Taffet SM, Delmar M, Spray DC. pH-dependent intramolecular binding and structure involving Cx43 cytoplasmic domains. *J Biol Chem*. 2002;277:36706–36714.

37. Stoyanovsky DA, Tyurina YY, Tyurin VA, Anand D, Mandavia DN, Gius D, Ivanova J, Pitt B, Billiar TR, Kagan VE. Thioredoxin and lipoic acid catalyze the denitrosation of low molecular weight and protein S-nitrosothiols. *J Am Chem Soc*. 2005;127:15815–15823.

38. Bateman RL, Rauh D, Tavshanjian B, Shokat KM. Human carbonyl reductase 1 is an S-nitrosoglutathione reductase. *J Biol Chem*. 2008;283:35756–35762.

39. Lamboley M, Pittet P, Koenigsberger M, Sauser R, Beny JL, Meister JJ. Evidence for signaling via gap junctions from smooth muscle to endothelial cells in rat mesenteric arteries: possible implication of a second messenger. *Cell Calcium*. 2005;37:311–320.

40. Sandow SL, Garland CJ. Spatial association of K-Ca and gap junction connexins in rat mesenteric artery. *FASEB J*. 2006;20:A275–A275.

41. Kameritsch P, Khandoga N, Nagel W, Hundhausen C, Lidington D, Pohl U. Nitric oxide specifically reduces the permeability of Cx37-containing gap junctions to small molecules 19. *J Cell Physiol*. 2005;203:233–242.

42. McKinnon RL, Bolon ML, Wang HX, Swarbreck S, Kidder GM, Simon AM, Tyml K. Reduction of electrical coupling between microvascular endothelial cells by NO depends on connexin37. *Am J Physiol Heart Circ Physiol*. 2009;297:H93–H101.

43. Retamal MA, Cortes CJ, Reuss L, Bennett MV, Saez JC. S-nitrosylation and permeation through connexin 43 hemichannels in astrocytes: induction by oxidant stress and reversal by reducing agents. *Proc Natl Acad Sci U S A*. 2006;103:4475–4480.

44. Retamal MA, Yin S, Altenberg GA, Reuss L. Modulation of Cx46 hemichannels by nitric oxide. *Am J Physiol Cell Physiol*. 2009;296:C1356–C1363.

45. Liu L, Hausladen A, Zeng M, Que L, Heitman J, Stamler JS, Steverding D. Nitrosative stress: protection by glutathione-dependent formaldehyde dehydrogenase. *Redox Rep*. 2001;6:209–210.